Article:

Bai, L orcid.org/0000-0001-9016-1569, Lin, G, Zhang, H et al. (1 more author) (2014) Effect of evaporator tilt on the operating temperature of a loop heat pipe without a secondary wick. International Journal of Heat and Mass Transfer, 77. pp. 600-603. ISSN 0017-9310

https://doi.org/10.1016/j.ijheatmasstransfer.2014.05.044

Effect of evaporator tilt on the operating temperature of a loop heat pipe without a secondary wick

Lizhan Bai[1,*], Guiping Lin[1], Hongxing Zhang[2], Dongsheng Wen[3]

1 Laboratory of Fundamental Science on Ergonomics and Environmental Control, School of Aeronautic Science and Engineering, Beihang University, Beijing 100191, PR China

2 Laboratory of Space Thermal Control Technology, Beijing Institute of Spacecraft System Engineering, Beijing 100094, PR China

3 School of Process Environment and Materials Engineering, University of Leeds, Leeds, LS2 9JT, UK

Abstract: The effect of evaporator tilt on the operating temperature of a loop heat pipe (LHP) without a secondary wick under terrestrial surroundings was investigated both experimentally and theoretically in this work. The experiments were conducted with the evaporator placed at three different tilts: (i) the evaporator was horizontal with the compensation chamber (CC), (iii) the evaporator was vertically below the CC, and (iii) the evaporator was higher the CC with a tilt angle of xx. The experimental results show that the evaporator tilt has significant effect on the operating temperature of the LHP: the operating temperature of the case iii) was much higher than the other two cases. A mathematical model including a two-zoned evaporator wick, i.e. a subcooled zone and a saturated zone, was built and solved, which agreed well with the experimental observation. . The results showed that the cooling effect of the returning liquid on the vapor region in the CC or evaporator core is crucial in determining the operating temperature of LHPs..

Keywords: loop heat pipe; evaporator tilt; operating temperature; heat leak; cooling effect

* Corresponding author. Tel.: +86 10 8233 8600; Fax: +86 10 8233 8600
E-mail address: bailizhan@buaa.edu.cn (L. Bai).

1 INTRODUCTION

Loop heat pipes (LHPs) are effective and efficient two-phase heat transfer devices that utilize the evaporation and condensation of a working fluid to transfer heat, and the capillary forces developed in fine porous wicks to circulate the working fluid [1, 2]. Their high pumping capability, excellent heat transfer performance and flexible thermal link function have been traditionally utilized to address the thermal-management problems of spacecraft, and successfully applied in many space tasks [3-11]. With the continuous development of LHP technology in space applications, more recently, its application has been extended to terrestrial surroundings such as in high heat flux electronics cooling [12-16] and thermal-management systems for aircraft and submarines [17-20].

For space applications, the effect of gravity on the operating characteristics of the LHP can be generally ignored due to the microgravity environment. The operating temperatures of the LHP are almost identical when the components are placed at different relative orientations. However for terrestrial applications, the liquid/vapor distribution and bubble movement in the two-phase components, and the gravitational pressure loss/gain in the system are strongly influenced by the gravity. The relative position of different components would affect significantly the heat and mass transfer processes, and result in different start-up and steady-state operation characteristics of the LHP.

So far, there have been quite a few literatures that reported the operation characteristics of LHPs on the ground, which showed their capability of transporting heat over a long distance under antigravity conditions and revealed their transient startup and power cycling characteristics [21-24]. It has been found that the relative orientation of the components has significant effect on the startup and steady-state performance of LHPs under terrestrial surroundings, which is briefly reviewed here.

Wolf et al.(1994) experimentally investigated the effect of adverse elevation, i.e., the evaporator is located above the condenser, on the operating temperature of a LHP in ground operation [21]. The results showed that the LHP operating temperature increased with increasing adverse elevations at low heat loads, being 8 K higher as the adverse elevations increased from 0.91 m to 2.74 mat a heat load of 25W. Such a operating temperature difference decreased with the increase of the heat load, and became indiscernible at heat loads over 200 W. Kaya et al. (2000) experimentally investigated the thermal performance characteristics of a terrestrial LHP with a large adverse elevation [22] aiming to transfer the excess heat from an electronic transformer to the underground. , Several tests were conducted including start-up, power cycling, and low and high-power tests to demonstrate its feasibility. The LHP demonstrated a heat transport capability of over 1kW at an adverse elevation of 4 meters. However, once deprimed??, the LHP would operate at a much higher temperature even after the evaporator power was reduced. In addition, some temperature fluctuation patterns were also observed. Zhang et al.(2005) experimentally investigated the effect of adverse elevation on the startup characteristics of an ammonia-stainless steel LHP in ground operation [23]. Experimental results showed that the adverse elevation had two-sided effects on the startup. On one hand, the additional pressure drop caused by the adverse elevation required a larger temperature difference across the evaporator wick, which caused a longer startup time and higher startup temperature. On the other hand, the possible presence of vapor bubbles in the vapor grooves of the evaporator due to the buoyancy effect could promote evaporation or boiling in the evaporator during the startup, which contributed to rapid working fluid circulation along the loop and reduction of the evaporator superheat. Chen et al. (2006) experimentally tested a miniature loop heat pipe under horizontal and four vertical orientations, i.e. “condenser above evaporator”, “evaporator above condenser”, “compensation chamber (CC) above evaporator” and “evaporator above CC” at various heat sink temperatures for electronic cooling applications [24] . The steady-state operating characteristics were similar for most of the orientations except for the one where the evaporator was above the compensation chamber. In fact, for the orientation “evaporator above CC”, the LHP didnot work at all for different heat sink temperatures. In general, the LHP can be started with very low power input (5W). There was a small temperature overshoot during start-up, which can be attributed to the slow movement of the cold liquid from the condenser. The start-up difficulty was encountered under two orientations, i.e., “condenser above evaporator” and “evaporator above condenser”.

As briefly reviewed above, the effect of relative positions between different components on the operation of LHPs under terrestrial surroundings has been extensively studied, however, the effect of evaporator tilt on the operating characteristics of LHPs is seldom reported , and little is known about the physical mechanisms associated with the evaporator tilt effect, which will be the main focus of this paper.

2 EXPERIMENTAL SETUP

A typical LHP consists of an evaporator, a condenser, a compensation chamber (CC) and vapor and liquid transport lines. The detailed structure of the evaporator and CC is shown in Fig.1, and Fig.2 shows the schematic view of a LHP. The experimental LHP was made of stainless steel except that the wick was made of sintered nickel powder, and Table 1 shows the basic parameters of the components where OD and ID represent the outer and inner diameters respectively. No secondary wick was employed in the ground tests, and the LHP had a bayonet extending to the middle point of the evaporator core. Ammonia was selected as the working fluid due to its excellent thermophysical properties in the temperature range of 0-60 ^{o}C.

Fig.3 shows the experimental setup. In the experiments, heat load applied to the evaporator was provided by a thin-film electric heater with the electric resistance of 20 Ω, attached directly to the evaporator casing symmetrically. The heat load can be adjusted from 0W to 300W by altering the DC power supply. The condenser line was mounted on an aluminum cold plate with imbedded coolant channels. Ethanol was used as the coolant for the condenser and circulated by a pump though a refrigerator. The heat sink temperature was maintained at constant values. The entire loop was thermally insulated with sponge to reduce the parasitic heat load from the ambient.

The data acquisition system composed of a data logger linked to a PC and the IMPview software was used to display and store the experimental data. Copper/constantan (Type T) thermocouples (TCs) were used to monitor the temperature profile along the loop, and the TC locations are shown in Fig.3. The vapor line was divided into four equal segments by the five TCs attached on it; and the condenser line was divided into five equal segments by four TCs attached on it. One additional TC was used to measure the ambient temperature (not shown in Fig3).

3 EXPERIMENTAL RESULTS AND ANALYSIS

3.1 Experimental results

In the experiments, the evaporator was placed at three different tilts: (a) the evaporator was horizontal with the CC; (b) the evaporator was vertically below the CC and (c) the evaporator was 6mm higher than the CC, as shown in Fig.4. In this section, the experimental conditions were maintained as follows: the ambient and heat sink temperatures were 21 ± 1^{o}C and -20 ± 0.5^{o}C respectively, and the evaporator and condenser were in a horizontal plane, i.e. no adverse elevation existed.

Fig.5 shows the heat load dependence of the operating temperature of the LHP when the evaporator was at tilts (a) and (b). As shown in Fig.5, when the evaporator was at tilt (a), the operating temperature of the LHP dropped gradually as the heat load applied to the evaporator increased from 20 to 200W, indicating that the LHP was operating in the variable conductance mode. The thermal conductance of the LHP increased continuously with the increase of the heat load. When the heat load applied to the evaporator was greater than 200W, the operating temperature of the LHP began to increase with the heat load, indicating that the LHP was operating in the constant conductance mode, i.e., the thermal conductance of the LHP remained almost invariant. The formation of variable conductance mode of the LHP is mainly caused by the parasitic heat load from the ambient, the adverse elevation and the variation of thermal conductance between the evaporator and CC, consistent with many previous reports. Similar phenomena were observed when the evaporator was at tilt (b), albeit the operation temperature in the variable conductance mode was a slightly lower than the tilt (a) case. In the constant conductance mode, the operating temperature difference between the two evaporator tilts reduced, and the two operating temperature curves almost overlapped.

Fig.6 shows the heat load dependence of the operating temperature when the evaporator was at tilts (a-c)., For the tilt (c), the general operation temperature dependence on the heat load is similar to that of (a) and (b), however it has some distinctive differences. The operating temperature at tilt (c) case was much higher than those when the evaporator was at tilts (a) and (b) in both operational modes, especially when the heat load applied to the evaporator was small (<100W). In fact when the heat load was smaller than 20W, the LHP was very difficult to start up and the evaporator temperature rose continuously even after 85℃. The system had to be shut down immediately before a steady state was reached for the safety purpose. For the case (c), the transition between the two operational models occurred ~ 100 W, which is much lower heat loads comparing the other two. Consequently, the evaporator temperature keeps decreasing for the tilt (c) between 100 and 200 W, while it starts to increase for the case of (a) and (b). Such experimental observation will be analyzed theoretically in the next section.

3.2 Theoretical analysis

The experimental results above shows clearly that the evaporator tilt has significant effect on the operating temperature of the LHP under terrestrial surroundings. For LHPs, the heat load applied to the evaporator (Q_{ap}) can be generally divided into three parts: i) the evaporative heat load, Q_e, which is applied at the outer surface of the evaporator wick and shares the majority of the total heat load. It can be expressed by Eq.(1):

$$Q_e = \dot{m}_e \cdot \lambda \tag{1}$$

ii) the heat leak from the evaporator to the CC, Q_{hl}, , , which includes the axial and radial contributions :

$$Q_{hl} = Q_{hla} + Q_{hlr} \tag{2}$$

and iii) the sensible heat the liquid passing through the wick, Q_{hw}, which increases the liquid's temperature to the evaporating temperature. Therefore the heat load applied to the evaporator can be expresses as:

$$Q_{ap} = Q_e + Q_{hl} + Q_{hw} \tag{3}$$

To the best of our knowledge, in the mathematical modeling or thermal analysis of the evaporator and CC of LHPs, most of the researchers consider that the working fluid in the evaporator core and the CC has a uniform temperature, i.e. the saturated temperature of the CC corresponding to the local pressure. For the simplification consideration, the heat leak from the evaporator to the CC is balanced by the subcooling of the returning liquid, neglecting the small heat transfer between the CC and the ambient [25-32]:

$$Q_{hl} = Q_{sub} \tag{4}$$

where

$$Q_{sub} = \dot{m}C_{pl}\Delta T_{sub} = \dot{m}C_{pl}(T_{cc} - T_{cc,in}) \tag{5}$$

If this assumption is true, the operating temperatures of the LHP at different evaporator tilts should be the same, which obviously conflicts with the experimental results presented above and in other literatures. In addition, this assumption doesn't take into account the effect of the compensation chamber geometry, which may also affect the heat and mass transfer in the evaporator and CC and eventually lead to different operating temperatures of the LHP [33].

To improve the mathematical modeling, both the temperature non-uniformity of the working fluid in the evaporator core and CC, and the cooling effect of the returning liquid are considered in this paper. Consequently, the inner surface of the evaporator wick is divided into a subcooled zone ($S_{wi,sub}$) and a saturated zone ($S_{wi,sat}$) according to the specific cooling condition of the returning liquid. In the subcooled zone, the working fluid is in the subcooled state without any bubble production from the inner surface of the wick. In the saturated zone, the working fluid is in the saturated state and bubbles appear continuously at the inner surface of the wick. Such a division is supported by our previous observations that bubble generation in some part of the inner surface of the evaporator wick was a common phenomenon. , For instance, Fig.7 shows the continuous bubble generation from the evaporator core and movement in the CC [34] for a LHP with dual CCs. Generally, the bubbles generated in the evaporator core will finally move into the vapor region in the CC due to the effects of the buoyancy fore and the entrainment of the fluid flow, and some bubbles may condense in this process due to the cooling effect of the returning liquid.

Based on the new model of heat and mass transfer in the evaporator and CC proposed above, the radial heat leak from the evaporator to the CC can be expressed as:

$$Q_{hlr} = Q_{hlr,sub} + Q_{hlr,sat} \tag{6}$$

where

$$Q_{hlr,sub} = G_{wi,sub}\left(T_e - T_{wi,sub}\right) \tag{7}$$

$$Q_{hlr,sat} = G_{wi,sat}\left(T_e - T_{cc}\right) \tag{8}$$

The radial heat leak from the evaporator to the CC in the subcooled region is balanced by the returning liquid flowing toward this region, resulting a lower temperature of the working fluid at the inner surface of the wick:

$$Q_{hlr,sub} = \dot{m}_{sub} C_{pl}\left(T_{wi,sub} - T_{bay,out}\right) \tag{9}$$

Quite different from the situation in the subcooled region of the inner surface of the evaporator wick, the radial heat leak from the evaporator to the CC in the saturated region consists of both sensible heat and latent heat due to the generation of bubbles there. The sensible heat leak in the saturated region is balanced by the returning liquid flowing toward this region:

$$Q^{s}_{hlr,sat} = \dot{m}_{sat} C_{pl}\left(T_{wi,sat} - T_{bay,out}\right) \tag{10}$$

and the latent heat leak from the evaporator to the CC in the saturated region is balanced by the heat transfer between the bubbles and the returning liquid, and between the vapor region and the returning liquid:

$$Q^{l}_{hlr,sat} = G_{bub}\left(T_{cc} - T_{bay,in}\right) + G_{vap}\left(T_{cc} - T_{bay,in}\right) \tag{11}$$

These two parts determine the required subcooled degree of the liquid at the CC inlet to establish stable liquid/vapor interface in the CC or the evaporator core. The better the heat transfer performance between the bubbles and the returning liquid and between the vapor region and the returning liquid, the smaller the required subcooling of the returning liquid, which can enhance the utilization efficiency of the condenser (α), i.e. the ratio between the two-phase area and the total area of the condenser, and lead to a lower operating temperature of the LHP, as shown by Eq.(12) [35]:

$$T_e = \left(\frac{dT}{dP}\right)_{sat} \times \left(\Delta P_{vg} + \Delta P_{vl}\right) + \frac{Q_e}{\alpha h_{c-s} A_c} + T_s \qquad (12)$$

When the evaporator is at tilt (a), the working fluid distribution and bubble movement in the evaporator and CC are schematically shown in Fig.8. Due to the jet impingement effect of the subcooled liquid at the exit of the bayonet, the left half side of the inner surface of the evaporator wick becomes the subcooled zone where no bubble emerges; and the right half side of the inner surface of the evaporator wick becomes the saturated zone where the cooling effect of the returning liquid is relatively small. The generated bubbles in the saturated zone flows into the vapor region in the CC due to the effect of the buoyancy and the entrainment of the fluid flow. Some bubbles may be condensed in this process due to the cooling of the returning liquid. In addition, there exists heat transfer between the vapor in the CC and the returning liquid in the bayonet through a layer of liquid between them, and the vapor in the CC condenses continuously to maintain a stable liquid/vapor interface in the CC.

When the evaporator is at tilt (b), as shown schematically in Fig.9, the top half side of the inner surface of the evaporator wick becomes the saturated zone. Similarly generated bubbles flows upward into the vapor region in the CC due to the effects of the buoyancy and the entrainment of the fluid flow. In addition, there exists good heat transfer between the vapor in the CC and the returning liquid in the bayonet because the bayonet goes directly through the vapor region in the CC, which enables the vapor in the CC condenses continuously to maintain a stable liquid/vapor interface in the CC. Compared with the situation of tilt (a), the bubbles in the evaporator core enters the vapor region in the CC easierand the heat transfer between the vapor in the CC and the returning liquid in the bayonet is improved . Consequently the returning liquid has a better cooling effect on the evaporator core and CC, which results in a lower operating temperature of the LHP as shown in Fig. 5.

Fig. 10 shows schematically the case of tilt (c). As the evaporator is slightly higher than the CC, the bubbles generated in the evaporator core flow toward the top end of the evaporator core, and accumulate there , which is much different from the situations of tilts (a) and (b). Due to the jet impingement effect of the subcooled liquid at the exit of the bayonet, the top half side of the inner surface of the evaporator wick except the vapor region becomes the subcooled zone and the bottom half side of the inner surface of the evaporator wick is the saturated zone where the cooling effect of the returning liquid is weak. As no bubble enters the CC and the bayonet goes directly through the CC, the CC will always be flooded with liquid. For the vapor region in the evaporator core, evaporation occurs at the inner surface of the evaporator core, and the radial heat leak from the evaporator to the evaporator core is relatively large. At the same time, the cooling effect of the subcooled liquid on the vapor region in the evaporator core is reduced due to the blockage of liquid, a much larger subcooling of the returning liquid is required to balance the heat leak from the evaporator to the vapor region in the evaporator core. Consequently the subcooled zone in the condenser must increase significantly, resulting in a considerable reduction of the utilization efficiency of the condenser and the increase of the operating temperature of the LHP.

Such an analysis agrees qualitatively with the experimental results. Quantitatively, Fig.11 shows the temperature profile of the LHP at the heat load of 200W when the evaporator was at tilts (a) and (c), respectively. For the tilt (a), the temperature of the fourth TC on the condenser was close to the operating temperature, indicating the co-existence of two-phase working fluid. The utilization efficiency of the condenser was more than 80% due to the good cooling effect of returning fluid on the vapor region in the CC. While for the tilt (c), the temperature of the second TC on the condenser is significantly lower than the operating temperature, indicating a subcooled liquid status. The utilization efficiency of the condenser was less than 40% due to the worse cooling effect of returning liquid on the vapor region in the evaporator core.

Of particular note that when the evaporator is at tilt (c) and the heat load is very small, i.e. $\leq$20W, the mass flow rate of the returning subcooled liquid in the bayonet is rather small, so does the cooling effect of the returning liquid.

The heat leak from the evaporator to the vapor region in the evaporator core cannot be effectively cooled by the returning liquid, the operating temperature of the LHP rises continuously and cannot reach a steady state below a safety operating temperature, i.e. 80℃. Such a modeling result is consistent with the experimental observation.

4 CONCLUSIONS

The effect of three evaporator tilt, (i) the evaporator was horizontal with the compensation chamber (CC), (iii) the evaporator was vertically below the CC, and (iii) the evaporator was higher the CC with a tilt angle of xx, on the operating temperature of a loop heat pipe (LHP) without a secondary wick under terrestrial surroundings was experimentally investigated and theoretically analyzed The evaporator tilt was found to have significant effect on the operating temperature of the LHP, more specifically,

- The operation temperature of the LHP for the case i) and ii) are quite similar, with slight lower temperature for the case ii)
- The operation temperature for the case iii) was significantly higher than the other two cases, and the LHP was transited into the constant conductance model at much lower heat loads.
-
- A mathematical model was established by considering the evaporation wick into a subcooled and a saturated zone, which agreed with experimental results well.
- The cooling effect of returning liquid on the vapor region in the CC or evaporator core, which depends on the evaporator tilt, is crucial in determining the operating temperature. Insufficient cooling may lead to high operation temperature, even unsuccessful startup under low heat load conditions. .
- The evaporator tilt has significant effect on the working fluid distribution and bubble movement in the evaporator and CC, which should be considered carefully in the LHP design.

ACKNOWLEDGEMENT

This work was supported by the national natural science foundation of China. Project No.

Nomenclature

A	area （m^2）
C_p	specific heat（J/kg K）
G	thermal conductance (W/K)
h	heat transfer coefficient (W/m^2 K)
$\dot{m}$	mass flowrate（kg/s）
P	pressure（Pa）
Q	heat load（W）
T	temperature（℃）

Greek symbols

α	utilization efficiency
λ	latent heat（J/kg）

Superscript

l	latent heat
s	sensible heat

Subscript

ap	applied
bay	bayonet
bub	bubble
c	condenser
cc	compensation chamber
c-s	condenser and heat sink
e	evaporator or evaporation
hl	heat leak
hla	axial heat leak
hlr	radial heat leak
hw	heating in the wick
in	inlet
out	outlet
s	heat sink
sub	subcooling or subcooled
sat	saturation
vap	vapor region
vg	vapor groove
vl	vapor line
wi	wick

REFERENCES

[1] Y.F. Maidanik, S.V. Vershinin, V.F. Kholodov, et al., Heat Transfer Apparatus, United States Patent: 4515209, 1985

[2] J. Ku, Operating characteristics of loop heat pipes. SAE paper, No. 1999-01-2007, 1999

[3] Y.F. Maydanik, Loop Heat Pipes, Applied Thermal Engineering, 25(2005) 635-657

[4] G.H. Wang, D. Mishkinis, D. Nikanpour, Capillary heat loop technology: space applications and recent Canadian activities, Applied Thermal Engineering, 28 (2008) 284-303

[5] S. Launay, V. Sartre, J. Bonjour, Parametric analysis of loop heat pipe operation: a literature review, International Journal of Thermal Science, 46 (2007) 621-636

[6] L. Bai, G. Lin, D. Wen, et al., Experimental investigation of startup behaviors of a dual compensation chamber loop heat pipe with insufficient fluid inventory, Applied Thermal Engineering, 29 (2009) 1447-1456

[7] Y. Zhao, T. Yan, J. Liang, Experimental study on a cryogenic loop heat pipe with high heat capacity, International Journal of Heat and Mass Transfer 54 (2011) 3304-3308

[8] P. Gully, Q. Mo, T. Yan, et al. Thermal behavior of a cryogenic loop heat pipe for space application, Cryogenics, 51 (2011) 420-428

[9] L. Bai, G. Lin, H. Zhang, et al. Experimental study of a nitrogen-charged cryogenic loop heat pipe, Cryogenics, 52 (2012) 557-563

[10] L. Bai, G. Lin, H. Zhang, et al. Operating characteristics of a miniature cryogenic loop heat pipe. International Journal of Heat and Mass Transfer, 55 (2012) 8093-8099

[11] L. Bai, G. Lin, H. Zhang, et al. Effect of component layout on the operation of a miniature cryogenic loop heat pipe. International Journal of Heat and Mass Transfer, 60 (2013) 61-68

[12] V.G. Pastukhov, Y.F. Maydanik, C.V. Vershinin, et al., Miniature Loop Heat Pipes for electronics cooling, Applied Thermal Engineering, 23(2003) 1125-1135

[13] V.G. Pastukhov, Y.F. Maydanik, Low-noise cooling system for PC on the base of Loop Heat Pipes, Applied Thermal Engineering, 27(2007) 894-901

[14] Y.F. Maydanik, S.V. Vershinin, M.A. Korukov, et al., Miniature loop heat pipes-a promising means for cooling electronics, IEEE transaction on Components and Packaging Technology, 28(2005) 290-296

[15] V.G. Pastukhov, Y.F. Maydanik, Active coolers based on copper-water LHPs for desktop PC, Applied Thermal Engineering, 29(2009) 3140-3143.

[16] J. Li, D. Wang, G.P. Peterson, Experimental Studies on a High Performance Compact Loop Heat Pipe with Flat Square Evaporator for High Power Chip Cooling, Applied Thermal Engineering, 30(2010) 741-752

[17] A.L. Phillips, K.L. Wert, Loop Heat Pipe Anti Icing System Development Program Summary, SAE paper, No.2000-01-2493, 2000

[18] A.L. Phillips, N.J. Gernert, Passive Aircraft Anti Icing System Using Waste Heat, SAE paper, No.981542, 1998

[19] N.J. Gernert, G.J. Baldassarre, J. Gottschlich, Loop Heat Pipes for Avionics Thermal Control, SAE paper, No. 961318, 1996

[20] J. Thayer, G. Hall, Flexible Air Cooled Loop Heat Pipe for High Density Avionics Cooling, AIAA paper, No. 2006-3413, 2006

[21] D.A. Wolf, W.B. Bienert, Investigation of Temperature Control Characteristics of Loop Heat Pipes, SAE paper, No.941576, 1994

[22] T. Kaya, J. Ku, Performance characteristics of a terrestrial loop heat pipe, AIAA paper, No.2000-0966, 2000

[23] Hongxing Zhang, Guiping Lin, Ting Ding, et al., Investigation of Startup Behaviors of a Loop Heat Pipe, Journal of Thermophysics and Heat Transfer, 19(4)(2005) 509-518

[24] Yuming Chen, Manfred Groll, Rainer Mertz, et al., Steady-state and transient performance of a miniature loop heat pipe, International Journal of Thermal Sciences 45 (2006) 1084-1090

[25] T. Kaya, T.T. Hoang, J. Ku, Mathematical Modeling of Loop Heat Pipes, AIAA paper, No. 99-0477, 1999

[26] T.T. Hoang, T. Kaya, Mathematical Modeling of Loop Heat Pipes with Two-phase Pressure Drop, AIAA paper, No. 99-3448, 1999

[27] J. Ambrose, E. Buchan, B. Yendler, Modeling and Test Results for a Loop Heat Pipe with Parallel-Flow Condenser, AIAA paper, No. 2000-2280, 2000

[28] M.L. Parker, Modeling of Loop Heat Pipe with Applications to Spacecraft Thermal Control, Pennsylvania: Faculty of Mechanical Engineering and Applied Mechanics, University of Pennsylvania, United States, 2000

[29] P.A. Chuang, J.M. Cimbala, C.T. Conroy, et al., Comparison of experiments and 1-D steady-state model of a loop heat pipe, Proceedings of IMECE, New Orleans, LA USA, 17-22 November, No. 2002-33542

[30] T.T. Hoang, T.A. O'Connell, J. Ku, Mathematical modeling of loop heat pipes with multiple capillary pumps and multiple condensers, Part I – steady state simulations, AIAA paper, No. 2004-5577, 2004

[31] V.V. Vlassov, R.R. Riehl, Mathematical model of a loop heat pipe with cylindrical evaporator and integrated reservoir, Applied Thermal Engineering, 28(2008), 942-954

[32] L. Bai, G. Lin, H. Zhang, et al. Mathematical modeling of steady state operation of a loop heat pipe, Applied Thermal Engineering, 29 (2009),2643-2654

[33] Roger R. Riehl, Tulio C.P.A. Siqueira, Heat transport capability and compensation chamber influence in loop heat pipes performance, Applied Thermal Engineering 26 (2006) 1158-1168

[34] G. Lin, N. Li, L. Bai, et al. Experimental investigation of a dual compensation chamber loop heat pipe. International Journal of Heat and Mass Transfer, 53(2010) 3231-3240

[35] M.A. Chernysheva, S.V. Vershinin, Y.F. Maydanik, Operating temperature and distribution of a working fluid in LHP, International Journal of Heat and Mass Transfer 50 (2007) 2704-2713

Table captions

Table1 Basic parameters of the LHP

Figure captions

Fig.1 Detailed structure of the evaporator and CC

Fig.2 Schematic of a LHP

Fig.3 Schematic of the experimental system

Fig.4 Three evaporator tilts in the experiments

Fig.5 Heat load dependence of the operating temperature at evaporator tilts (a) and (b)

Fig.6 Heat load dependence of the operating temperature at evaporator tilts (a-c)

Fig.7 Bubble generation and movement in the CC

Fig.8 Working fluid distribution and bubble movement in the evaporator and CC at evaporator tilt (a)

Fig.9 Working fluid distribution and bubble movement in the evaporator and CC at evaporator tilt (b)

Fig.10 Working fluid distribution and bubble movement in the evaporator and CC at evaporator tilt (c)

Fig.11 Temperature profile of the LHP at the heat load of 200W

Table1 Basic parameters of the LHP

Components		Dimensions
OD/ID×Length of Evaporator		Φ18/16×175mm
OD/ID×Length of Condenser		Φ3/2.2×2000mm
Vapor/liquid line length		2800/2500mm
OD/ID of vapor and liquid line		3/2.2mm
Width/height×number of vapor grooves		1.5/1.2mm×20
Volume of CC		20ml
Charge of working fluid		29.9g
Wick	OD/ID×length	16/8×125mm
	Maximum radius	1.0μm
	Porosity	58.7%
	Permeability	$>5\times10^{-14}m^2$

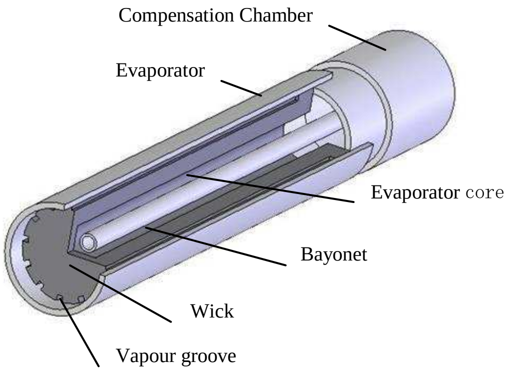

Fig.1 Detailed structure of the evaporator and CC

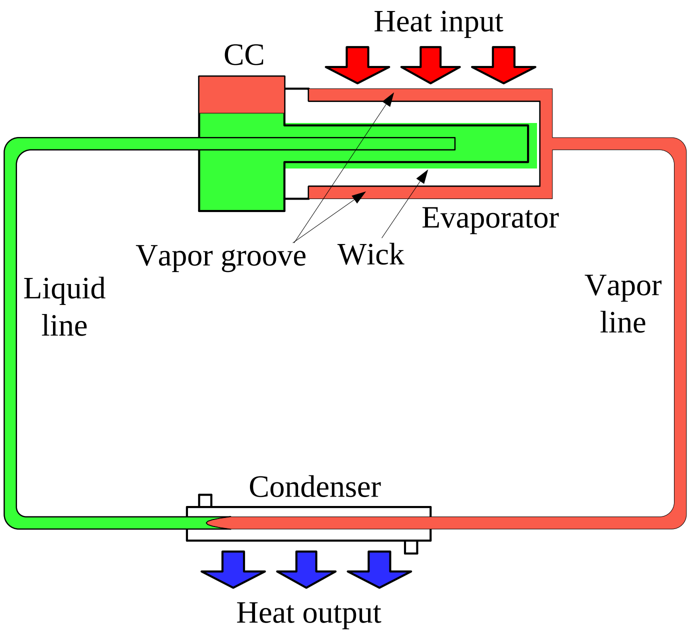

Fig.2 Schematic of a LHP

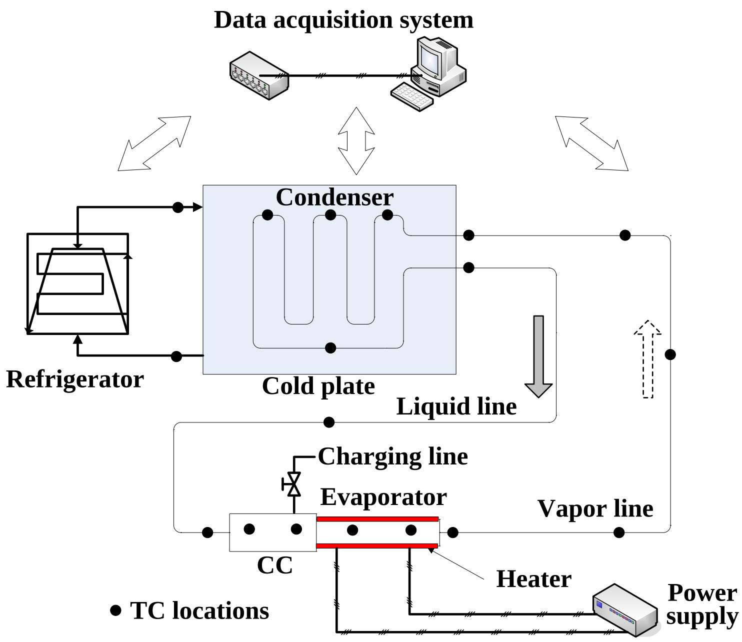

Fig.3 Schematic of the experimental system

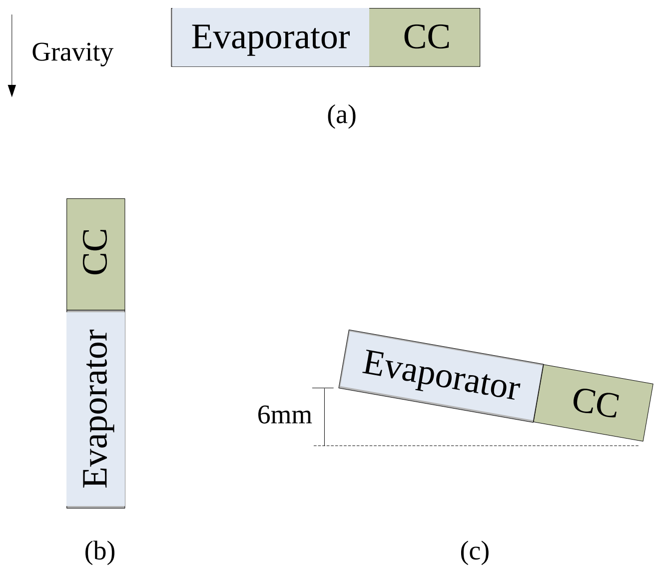

Fig.4 Three evaporator tilts in the experiments

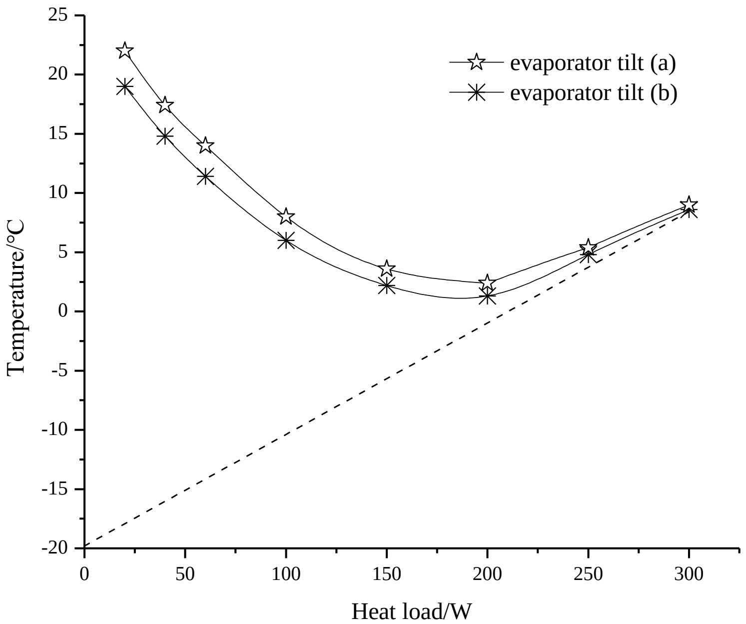

Fig.5 Heat load dependence of the operating temperature at evaporator tilts (a) and (b)

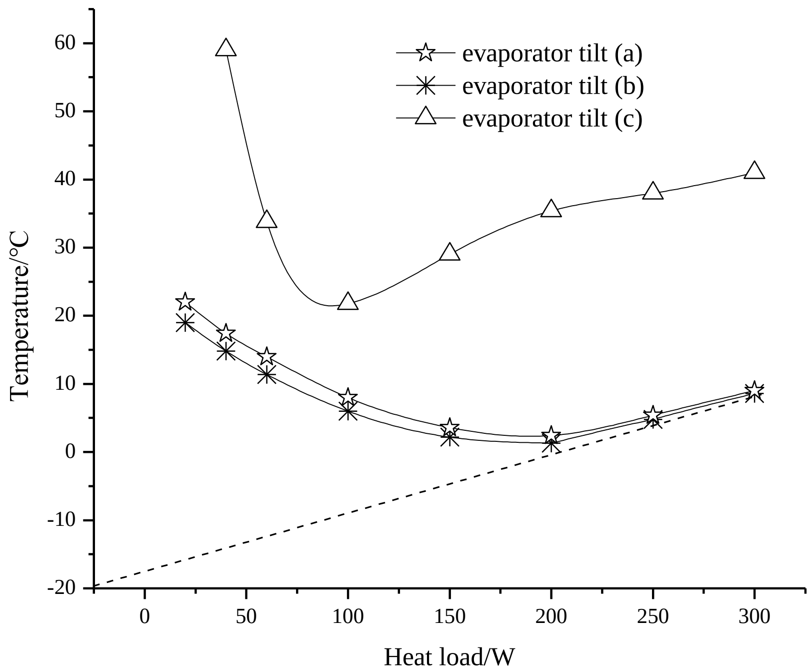

Fig.6 Heat load dependence of the operating temperature at evaporator tilts (a-c)

Fig.7 Bubble generation and movement in the CC [34]

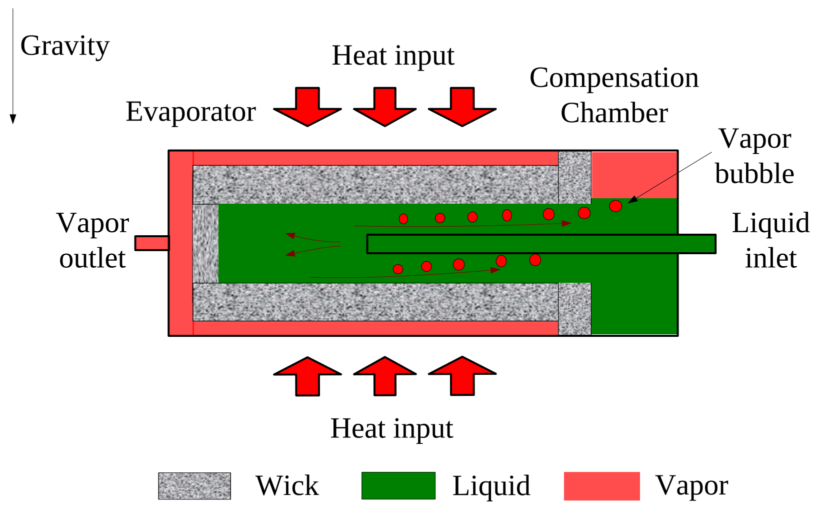

Fig.8 Working fluid distribution and bubble movement in the evaporator and CC at evaporator tilt (a)

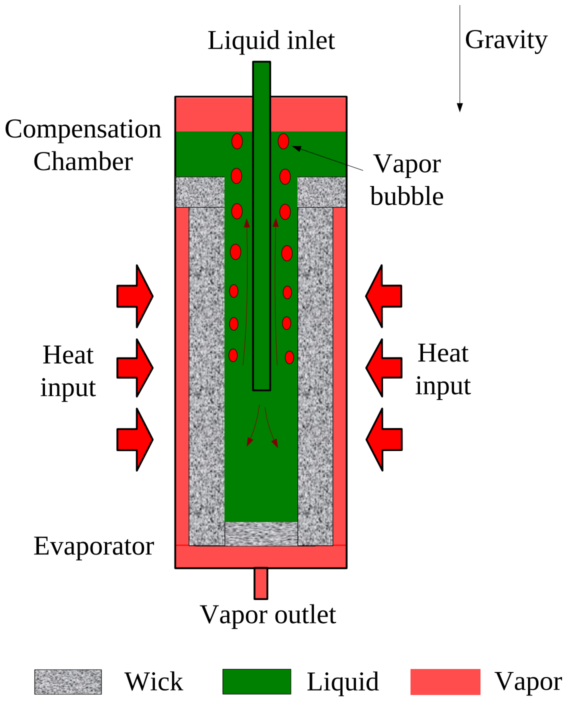

Fig.9 Working fluid distribution and bubble movement in the evaporator and CC at evaporator tilt (b)

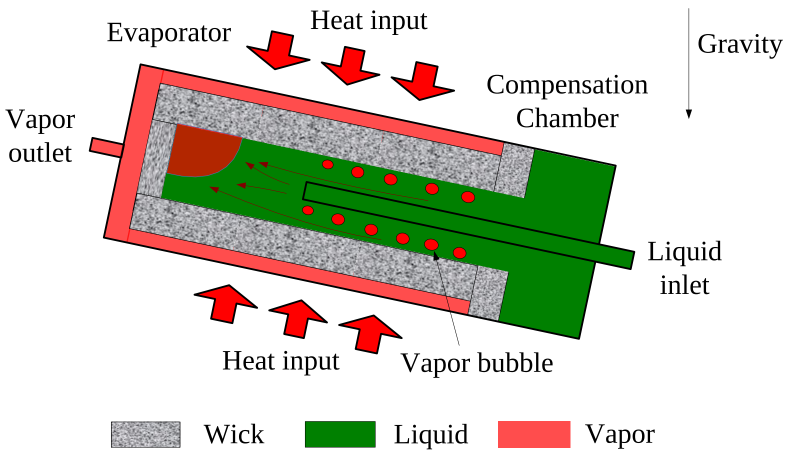

Fig.10 Working fluid distribution and bubble movement in the evaporator and CC at evaporator tilt (c)

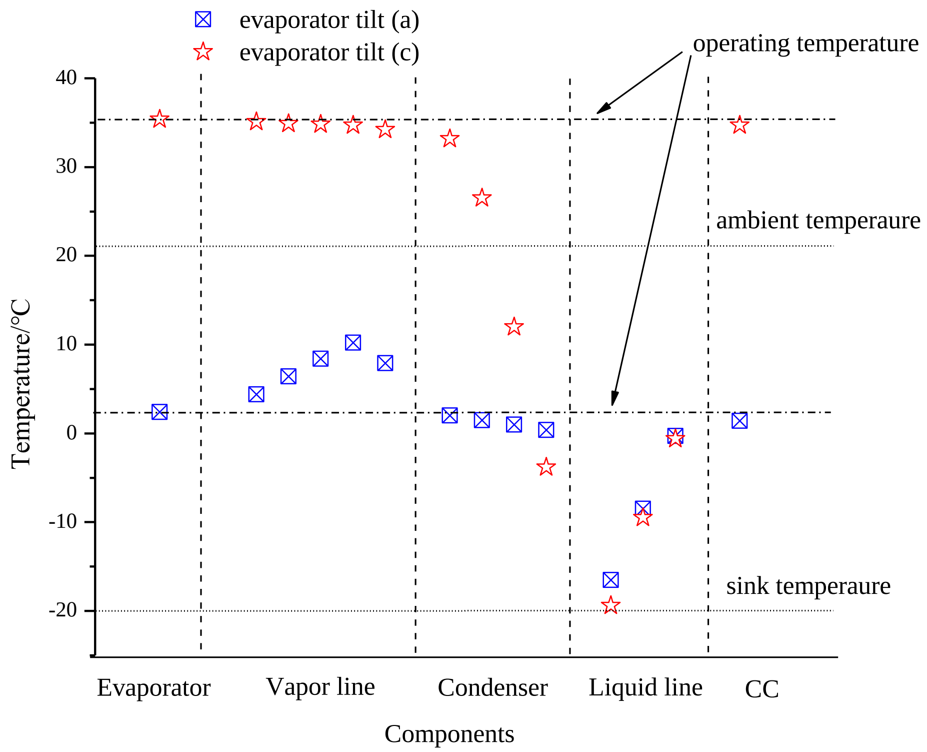

Fig.11 Temperature profile of the LHP at the heat load of 200W